

3. Beam Propagation Method Simulation

3.1 Modifications to Beam Propagation Method Simulation

For the Beam Propagation Method (BPM) simulation, we modified the refractive index profile of the waveguide to be a function of both x and z . A single for-loop is used to iterate over the z -steps and the corresponding refractive index profile as a function of x is determined. An offset is added to the mode converter, which determines where the perturbation starts along the z -axis. The index of the core is modified to be equal to the effective index obtained from the 1D thin waveguide cross section, as presented in Section 2.1.

```
counter = 0;
L = 1300*um;
A = 62.9898*um;
width_perturbation = 0.1*um;
offset = 500; % Offset for where perturbation starts
for j = 1 : Nzpts + 1
    if (j < offset)
        coreinds = find((x<=inputWGWidth/2).*(x>=-inputWGWidth/2));
        n_Input_WG(j,coreinds) = nCore;
        continue
    end
    if((counter<(A/deltaz)*0.5)&&(j<L/deltaz + offset))
        coreinds = find((x<=inputWGWidth/2).*(x>=-inputWGWidth/2));
        n_Input_WG(j,coreinds) = nCore;
        perturbationinds = coreinds(1:round(width_perturbation/deltax));
        n_Input_WG(j,perturbationinds) = nCladding;
    else
        coreinds = find((x<=inputWGWidth/2).*(x>=-inputWGWidth/2));
        n_Input_WG(j,coreinds) = nCore;
    end
    if(counter>=(A/deltaz))
        counter = 0;
    end
    counter = counter+1;
end
```

Figure 7. Refractive Index Profile Code for the BPM Simulation

In addition, an input waveguide of length 500 μm consisting of the same width and core and cladding indices as the mode converter is added to the BPM simulation. This is added to give appreciable distance for the gaussian input source to excite the TE0 mode. The width of the input gaussian is tuned in order to lead to the greatest degree of TE0 excitation.

The Crank-Nicolson code in the simulation is modified to extract the index profiles at both z_m and z_{m+1} as the index is now a function of both x and z . In addition, a numerical overlap integral calculation is implemented at each z -step of the simulation in order to compute the TE0 and TE1 modal powers during propagation, using the current field profile as a function of x and the expected modal profile. The modal modal profiles were normalized such that the self-overlap integral is unity. The built-in MATLAB *trapz()* function is used for the numerical integration.

```

for m = 1 : Nzpts
    n_m_plus_1 = n_Input_WG(m + 1, :);
    n_m = n_Input_WG(m, :);
    b = (2*alpha)/(deltax^2) - alpha*(n_m_plus_1.^2 - kappa.^2 + ...
        2*1i*n_m_plus_1.*kappa - nBar^2)*k0^2 + 2*1i*k0*nBar/deltaz;

    r(1) = (1-alpha)/(deltax^2) * (0+u(2)) + ...
        ((1-alpha)*(n_m(1)^2-kappa(1)^2 + 2*1i*n_m(1)*kappa(1) - ...
        nBar^2)*k0^2 - 2*(1-alpha)/(deltax^2) + 2*1i*k0*nBar/deltaz) * u(1);
    r(N) = (1-alpha)/(deltax^2) * (u(N-1)+0) + ...
        ((1-alpha)*(n_m(N)^2-kappa(N)^2 + 2*1i*n_m(N)*kappa(N) - ...
        nBar^2)*k0^2 - 2*(1-alpha)/(deltax^2) + 2*1i*k0*nBar/deltaz) * u(N);
    for j = 2 : N-1
        r(j) = (1-alpha)/(deltax^2) * (u(j-1)+u(j+1)) + ...
            ((1-alpha)*(n_m(j)^2-kappa(j)^2 + 2*1i*n_m(j)*kappa(j)- ...
            nBar^2)*k0^2 - 2*(1-alpha)/(deltax^2) + 2*1i*k0*nBar/deltaz) * u(j);
    end
end

```

Figure 8. Crank-Nicolson Algorithm for the BPM Simulation

3.2 Beam Propagation Method Simulation Results

For our default test structure presented in Table 1 and Figure 4, the following simulation parameters are used in the BPM simulation.

Table 3. MATLAB BPM Simulation Parameters

n_{Cladding}	n_{Core}	Waveguide Length (μm)	Waveguide Width (μm)	Δz (μm)	Δx (μm)	Grating Period (μm)	Absorbing Edge Length (μm)	κ_{Max} (μm)
1.4459	1.52114	1500	4	0.25	0.01	62.9898	2	-0.03

The BPM simulation results are shown in Figure 9. The results include the E-field profile and the modal powers as a function of propagation distance.

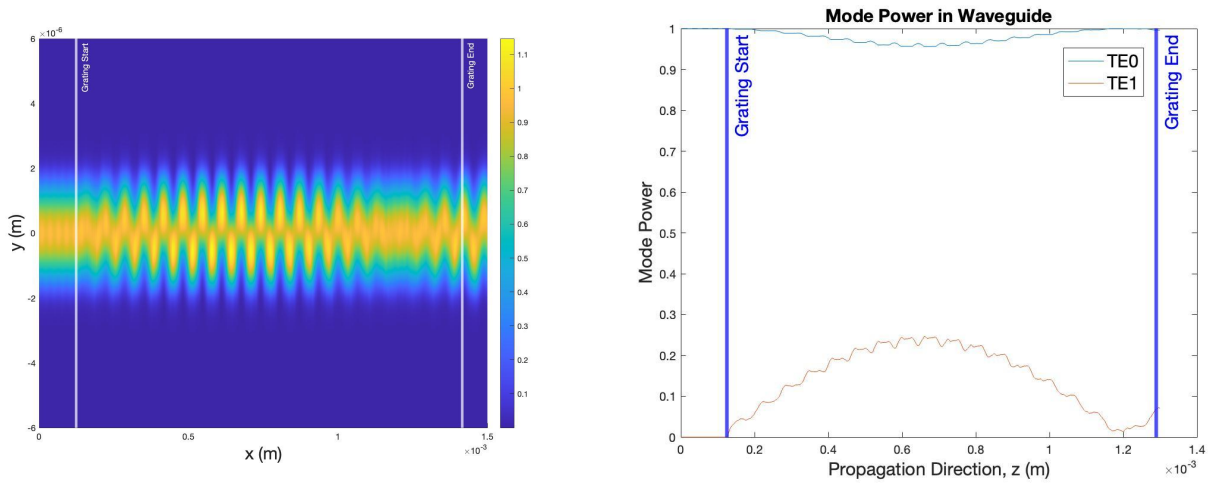


Figure 9. (a) E-field profile in x-y plane and (b) Modal power during propagation

In the BPM simulation, the input gaussian was passed through an input waveguide of length 500 μm with no perturbation. Then, the evolved profile was set as the input to the mode converter. The periodic grating in the mode converter starts at approximately 125 μm . As it propagates through the structure, a TE1 mode component starts to develop, as seen by the splitting of electric field amplitudes. However, there still is a noticeable electric field amplitude at $y = 0$, which is indicative of the presence of the fundamental mode. At 1 mm and beyond, the profile starts to evolve back towards the fundamental mode. These behaviors are supported by the modal power evolution in Figure 7b, which was computed using a numerical overlap integral. At 0.7 mm, the TE1 mode power reached a maximum value of 0.25 where the TE0 mode power reached a minimum value of 0.95. Beyond 0.7 mm, the TE1 and TE0 mode powers declined and increased, respectively.

As the BPM simulation was performed based on a structure developed using an incorrect design method, the device was not expected to be optimal at an operating wavelength of 1550 nm. In addition, since the BPM simulation was developed after the performance of the FDTD simulation, it was not used to optimize our design. However, the BPM simulation was used to analyze the dependence of modal power evolution as a function of critical parameters, which will be discussed in the “Discussion and Conclusion” section.

4. Test Structure Definition and Full-vectorial FDTD Simulation

4.1 FDTD Simulation Results

For the full-vectorial FDTD Simulation, the test structure used is shown in Figure 10.



Figure 10. (a) Full GDS test structure designed using KLayout; waveguide device has length of 1600 μm with 21 grating teeth and grating periodicity of 62.9898 μm



Figure 10. (b) Single grating teeth in the test structure

The electric field profile for the test structure obtained using FDTD is shown in Figure 11.

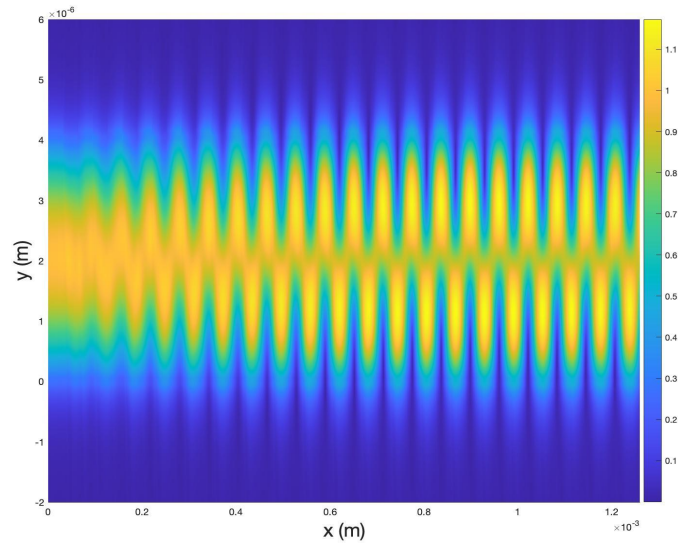


Figure 11. E-field in x-y plane obtained from FDTD Simulation

In addition, the reflection and the transmissions for the fundamental and first-order for the input to the mode converter are shown in Figure 12.

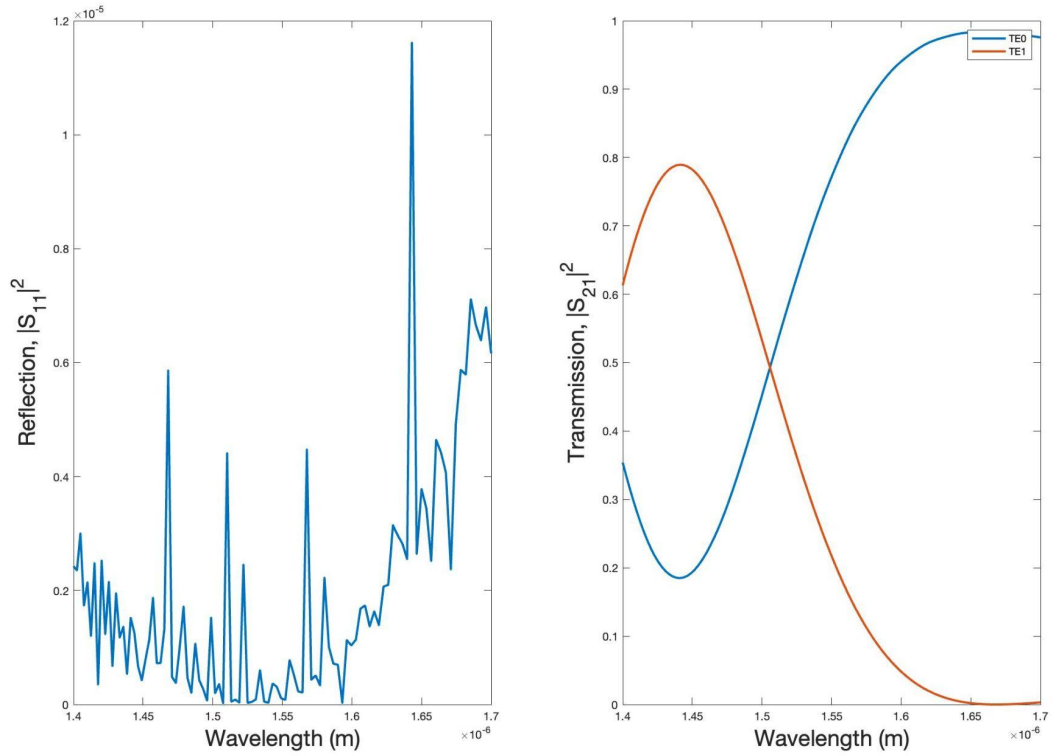


Figure 12. Reflection and transmissions for the TE0 and TE1 modes as a function of operating wavelength

Evidently, the performance of the mode converter is suboptimal at the intended operating wavelength of 1550 nm. The mode converter has a TE1 transmission of approximately 20% and TE0 transmission of approximately 80% at 1550 nm. The peak conversion efficiency is achieved at an operating wavelength of approximately 1440 nm, with a peak transmission of the TE1 mode of 79% and a minimum transmission of the TE0 mode of 19%. The mode converter also has minimum reflection at 1593 nm and 1507 nm. At 1550 nm, the device has a local minimum for reflection, while at 1440 nm, it has a local maximum. As our initial approach for the design of the mode converter was incorrect, with the modal analysis being the primary hindrance, we did not expect the device to perform optimally at the originally intended wavelength.

5. Discussion and Conclusion

5.1 Comparison between FDTD and BPM Simulation

When comparing the BPM to the FDTD simulations, there are clear differences between the two, as seen in Figure 13. The width of the individual electric field amplitude peaks for the BPM simulation are lower than that of the FDTD simulation. In addition, beyond approximately 1.1 mm along the propagation direction, the TE1-like mode starts to converge back towards the TE0 mode, as seen by the joining of the amplitude peak separation.

Generally, the BPM method is most suitable for structures with low Δn , which is the case with mode converter structure. The BPM simulation relied on the transformance from a 2D waveguide structure to an equivalent 1D waveguide structure using the effective index method. When looking at the aspect ratio of the device, the effective index is generally applicable as the aspect ratio is 8, which is sufficiently large. In addition, the grating tooth width is small enough such that there does not exist significant back reflection.

Some numerical rounding while solving the TE mode transcendental equation along the y-axis may have resulted in deviations from the true value, although the effects of this deviation is likely to be small. In addition, the validity of the effective index method in tandem with the BPM method should be further scrutinized.

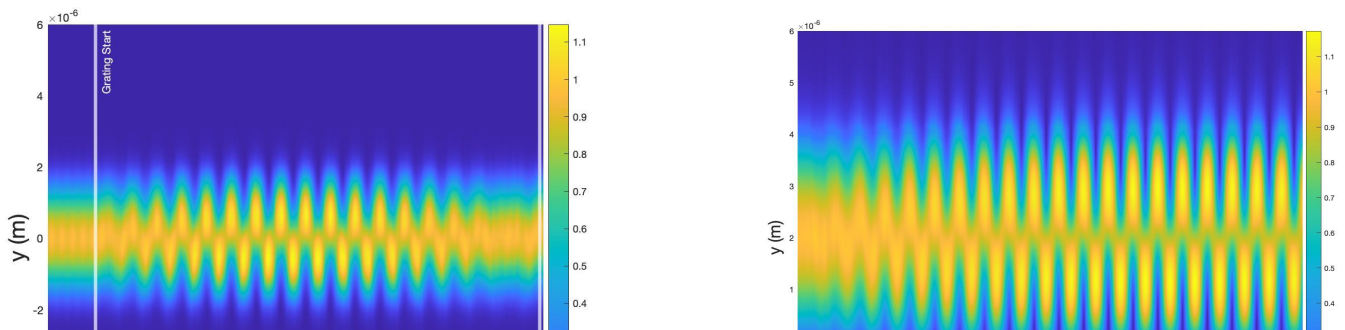


Figure 13. (a) BPM Simulation Results and (b) FDTD Simulation Results

5.2 Dependence on Critical Parameters

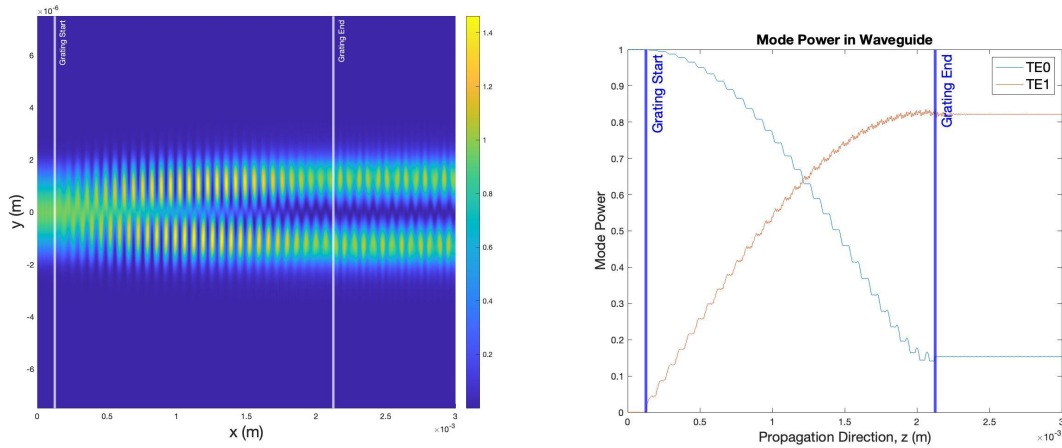


Figure 14. (a) E-field profile in x-y plane in the mode converter with device length of $3000 \mu\text{m}$, grating length of $2000 \mu\text{m}$, and periodicity of $66.5 \mu\text{m}$ and (b) Modal power during propagation

After many attempts of the BPM simulation, it was decided that an iterative process based on the tuning of critical parameters would result in the most rapid optimization. Beginning with the initial design of parameters in Table 1, a discretized optimization process was implemented to calculate the peak performance the initial design could achieve. This was done by discretizing the grating periodicity and iterating over a range of periodicity values of approximately 5% of the original, while simultaneously monitoring the TE1 mode power output.

During this process, it was discovered that increasing the grating length yielded higher TE1 mode output power. Beginning at the original grating length of $1300 \mu\text{m}$ and iterating over 100

μm steps while keeping other parameters constant, it was found that the peak grating length occurred at approximately $2000 \mu\text{m}$. This implies an inaccuracy in the original coupling coefficient for the waveguide as the grating length is only the resultant of the intermodal coupling. Equation 7 illustrates the output variation of grating length could be the result of a number of design parameters, including the perturbation depth, modal effective indices, gaussian profiles, and waveguide width. While it may be tempting to dive deeper into the tuning of these parameters, the resulting impact on the BPM functionality is too great and causes a collapse of intermodal coupling. It is more worthwhile to tune higher order geometries than the fundamental parameters that allow the BPM and coupling to function.

It can be seen in Figure 14 that for a grating periodicity of approximately $66.5 \mu\text{m}$ and length of approximately $2000 \mu\text{m}$, the output power in the TE1 mode has become 84% of the propagating energy. Compared to the initial performance, this corresponds to an increase in TE1 mode transmission by a factor of 4. Additionally, the increased length of the grating results in higher modal definition of the TE1 mode. Comparing Figure 9a) and Figure 14a), it is clear that the TE0 transmission is reduced at the output port.

The effects of grating tooth width was also analyzed on the minimum and maximum transmission of TE0 and TE1 modes. Transmission in the case refers to the minimum and maximum proportions of TE0 and TE1 modes along the propagation direction. In Figure 15, three different configurations for the tooth width are analyzed for a waveguide of length $3000 \mu\text{m}$ and grating length of $1425 \mu\text{m}$. For a given tooth width, there is an associated optimal grating period that yields the highest TE1 mode proportion of greater than 90%. As the tooth width is increased, the optimal grating period is reduced starting from $65 \mu\text{m}$ down to $62.5 \mu\text{m}$.

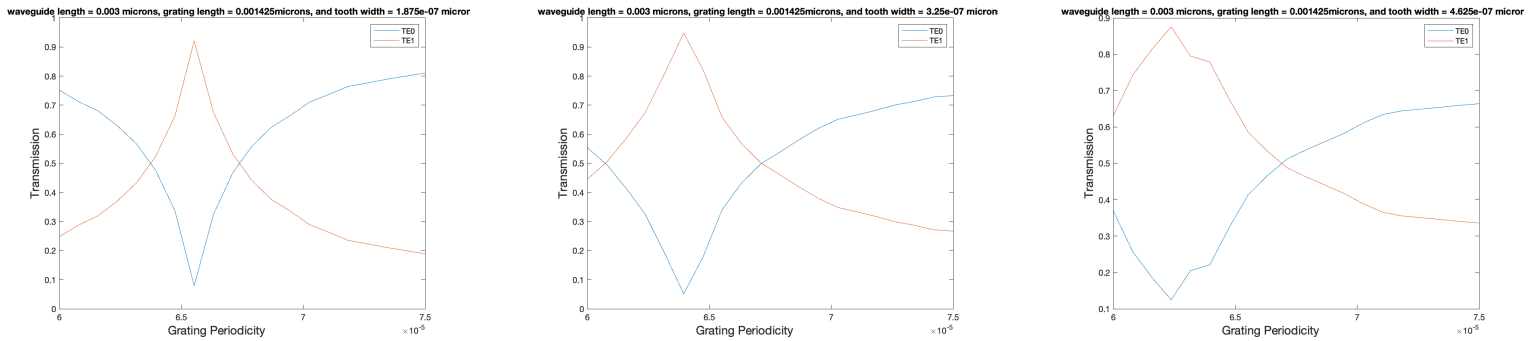


Figure 15. Minimum and Maximum Transmission of TE0 and TE1 Modes in Waveguide of length $3000 \mu\text{m}$ with (a) grating length = $1425 \mu\text{m}$, tooth width = $0.1875 \mu\text{m}$ (b) grating length = $1425 \mu\text{m}$, tooth width = $0.325 \mu\text{m}$ and (c) grating length = $1425 \mu\text{m}$, tooth width = $0.4625 \mu\text{m}$

In addition, the BPM simulations for the optimal grating periodicities at each tooth width are shown in Figure 16.

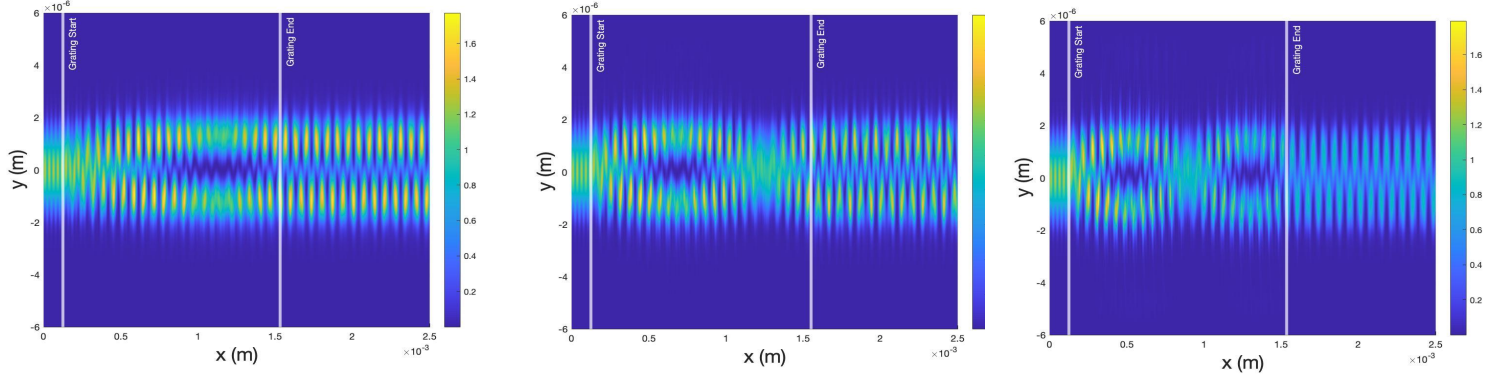


Figure 16. E-field Profile obtained via BPM Simulation in waveguide of length 3000 μm with (a) grating length = 1425 μm , tooth width = 0.1875 μm , periodicity = 66.5 μm (b) grating length = 1425 μm , tooth width = 0.325 μm , periodicity = 63.5 μm , and (c) grating length = 1425 μm , tooth width = 0.4625 μm , periodicity = 62.5 μm

The grating length of 1425 μm is compatible with the configuration of tooth width of 0.1875 μm with clear mode splitting from the TE₀ to the TE₁ mode. For the configuration of tooth width of 0.325 μm and tooth width of 0.4625 μm , the TE₁ mode starts to emerge at approximately 0.5 mm. However, beyond this point along the propagation direction, the emerging TE₁ mode starts to morph back into the TE₀ mode. Thus, in practice, the original grating length for both of these grating width configurations are longer than optimal and should be reduced such that the grating terminates at the highest proportion of the TE₁ mode.

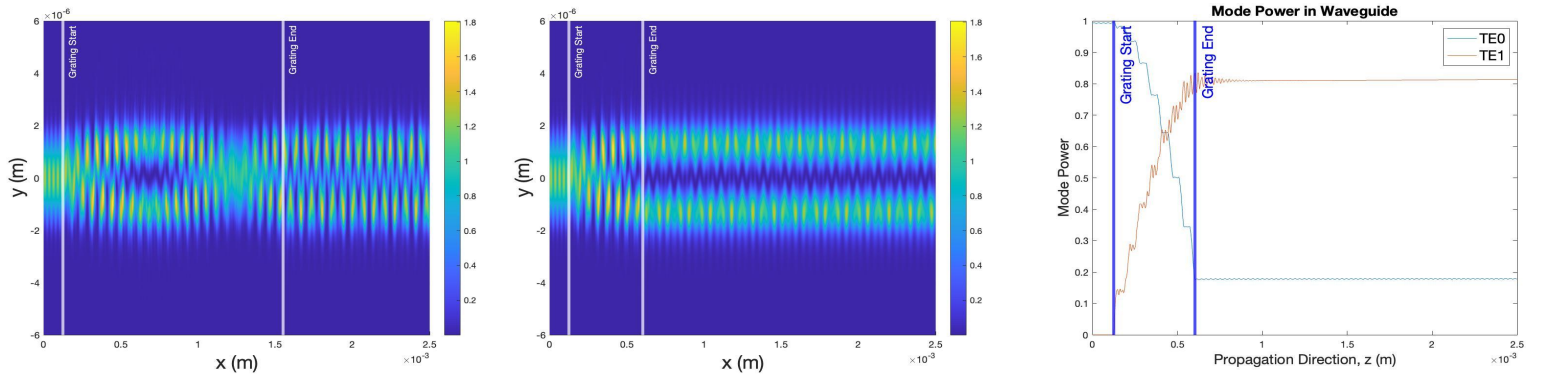


Figure 16. E-field Profile obtained via BPM Simulation in waveguide of length 3000 μm and periodicity of 63.5 μm with (a) grating length = 1425 μm , tooth width = 0.325 μm (b) shortened grating length = 500 μm , tooth width = 0.325 μm and (c) transmission of waveguide with shortened grating length

When the grating length is reduced to 500 μm , the mode splitting from the TE₀ to TE₁ mode is much more pronounced at the output port of the mode converter. The TE₁ transmission with this grating length reached approximately 80%, while the TE₀ transmission was reduced to under 20%.